G01

APPLICATION OF A NEW MULTIOBJECTIVE EVOLUTIONARY ALGORITHM TO THE OPTIMUM DESIGN OF A REMOTE SENSING SATELLITE CONSTELLATION

R. L. GALSKI[1], F. L. DE SOUSA[2] and F. M. RAMOS[3]

[1] *Centro de Rastreio e Controle de Satélites (CRC), Instituto Nacional de Pesquisas Espaciais (INPE), Av. dos Astronautas, 1758, São José dos Campos, SP, 12227-010, Brasil*, e-mail: galski@ccs.inpe.br

[2] *Divisão de Mecânica Espacial e Controle (DMC), Instituto Nacional de Pesquisas Espaciais (INPE), Av. dos Astronautas, 1758, São José dos Campos, SP, 12227-010, Brasil*, e-mail: fabiano@dem.inpe.br

[3] *Laboratório Associado de Computação e Matemática Aplicada (LAC), Instituto Nacional de Pesquisas Espaciais (INPE), Av. dos Astronautas, 1758, São José dos Campos, SP, 12227-010, Brasil*, e-mail: fernando@lac.inpe.br

Abstract. This paper describes an application of a multi-objective version of the Generalized Extremal Optimization (GEO) algorithm to the inverse design of a remote sensing satellite constellation. The GEO algorithm is a recently proposed global search method [14], [16], based on a model of natural evolution [1], and specially devised to be used in complex optimization problems. Easy to implement, GEO has only one free parameter to adjust, does not make use of derivatives and can be applied to constrained or unconstrained problems, non-convex or even disjoint design spaces, with any combination of continuous, discrete or integer variables. The multi-objective version of GEO presented here was developed to generate the Pareto frontier maintaining the GEO essence: universality of application and just one algorithm parameter to adjust. The application reported concerns the optimum design of a small constellation of MAPSAR (Multi-Application Purpose Synthetic Aperture Radar) satellites. The MAPSAR satellite program is a Brazilian-German joint project aimed at the assessment, management and monitoring of Earth's natural resources [12]. The design procedure is tackled as a multi-objective optimization problem, considering two major performance parameters, the average revisit time and the maximum revisit time over a region of interest. The revisit time is the metric traditionally used to evaluate sparse coverage constellations, e.g., constellations that do not achieve continuous coverage of an area on the Earth's surface. Trade-off studies are carried out for several numbers of satellites in the constellation, in order to access the best ratio between performance and cost.

1. INTRODUCTION

This paper addresses the optimum design of a satellite constellation for non-continuous coverage of a region of interest on the Earth's surface. The problem is posed as a two-objective optimization problem, where the maximum and the average revisit time over the interest region are the two objectives and some of the satellite ephemeris (inclination, right ascension and mean anomaly) are the design variables.

The constellation is based on the MAPSAR satellite. MAPSAR stands for Multi-Application Purpose Synthetic Aperture Radar and it is a Brazilian-German joint program, conducted by INPE (National Institute for Space Research) from Brazil and DLR (German Aerospace Center), whose aim is to obtain a satellite that allows the assessment, management and monitoring of natural resources [12].

The SAR (Synthetic Aperture Radar) sensor allows high-resolution imagery independently of weather or sun light, which is particularly important for regions that have the presence of rain, clouds, haze and smoke, like, for instance, the Amazon region.

The MAPSAR satellite has its launch foreseen to 2008, in a low-Earth sun-synchronous orbit. In April 2002, a working group of Brazilian SAR scientists and potential SAR end-users met on the campus of INPE (São José dos Campos) and it was strongly recommended that a series of such satellites should be built aiming at the operational aspects and the program continuity. More than that, the Brazilian and the German requirements specifically concerning disaster monitoring both state as desirable a revisit time lesser than one day [12]. The most recent information about the MAPSAR orbital characteristics points to a periodicity (revisit time) of 7 days, which does not match the user requirements for disaster monitoring. In this way, the present study of the design of a constellation of MAPSAR satellites can be relevant in the near future.

Considering the importance of remote disaster monitoring over a scarcely populated region, as is the Brazilian Amazon region, this paper tries to answer what is the best constellation configuration in order to achieve the smallest possible revisit time, while keeping one of the satellites in the original sun-synchronous orbit of MAPSAR, to maintain the global coverage feature.

It was pointed out recently that the maximum and the average revisit time of low-Earth orbit sparse coverage satellite constellations are aims that often compete with each other [17]. The revisit time lesser than one day requirement can be entirely fulfilled considering only the maximum revisit time as the objective for the optimum design. However, the average revisit time is also important as a performance measure of the constellation. Then, it was decided to consider both as objectives by conducting a multiobjective optimization in order to obtain the Pareto frontier [8].

In multiobjective optimization problems [8], [18], one wants to optimize (minimize or maximize) simultaneously a set of objectives. Normally, for these problems, there is not only one optimal design solution, but a family of compromise design solutions, that do not need to be global optima to any individual objective. Following the notion of Pareto optimization, this family is named the Pareto set or the Pareto optimal set and the corresponding points in the objective space are called the Pareto front (or the Pareto frontier) [18]. A feasible point in the objective space belongs to the Pareto frontier if none of the objectives can be further improved without worsening any of the other objectives. Any solution from the Pareto set can be used and it is a designer's task to choose which one will be implemented, based in the Pareto frontier itself or other factors.

There are, in the literature, many numerical techniques developed to deal with multiobjective optimization problems [11], [13], [2]. These techniques can be grouped basically into three approaches [5], [3].

One approach, referred to as aggregation methods, is to transform the multiobjective into a single-objective problem, by combining all objectives into one single-objective function, also denominated compromise function. The simplest example of such methods is the weighted sum approach, where the compromise function is a linear combination of the objectives. If the designer has the *a priori* information about which weights must be used, the problem is, in fact, single-objective and there is no need for finding the Pareto frontier. If it is not the case, the Pareto frontier is mapped by solving several times the single-objective problem, each time with a different set of weights (coefficients). The designer is free to choose the global optimization method of its preference to solve the (single) optimization problems. It is already known that this approach has not the ability to capture the entire Pareto frontier for problems with concave Pareto surfaces. It should be noticed, however, that the assembly of the single-objective function can be done by several ways, including non-linear ones, where the coefficients introduced alter the single-objective function curvature, thus allowing the capture of points of the Pareto frontier that could not be captured by the weighted sum approach. Based on this fact, several non-linear formulas have been developed. Reference [10] lists several aggregating function formulas that have been used so far and briefly comments its strengths and weaknesses, while reference [3] does it in a more extensive way but in the context of Multiobjective Evolutionary Algorithms (MEAs).

A second approach, known as Pareto-based approach, uses directly the non-dominance as a criterion to guide the search. Non-dominance is a concept from Pareto optimality. A feasible point in the objective space dominates others if it improves at least one of the objectives without worsening any of the others. This point is said to be a non-dominated point. Considering the entire feasible objective space, the set of all non-dominated points forms the Pareto frontier itself. By keeping a set of non-dominated points along the search, one gets an approximation of the Pareto Frontier. This approach was born inside the Multiobjective Evolutionary Algorithms (MEAs) branch of methods, where the non-dominance criterion was used to define the fitness function for Genetic Algorithms (GAs) [9]. Examples of algorithms based on this approach are the Multiple Objective Genetic Algorithm (MOGA), the Non-Dominated Sorting Genetic Algorithm (NSGA), and the Niched Pareto Genetic Algorithm (NPGA). References [3] and [18] analyze more deeply techniques based on this approach.

And the third approach, referred to as non-Pareto approach, fills the complementary set, regarding the first two approaches. It groups together all the methods that use neither the aggregation approach nor the Pareto approach. Examples of algorithms based on this approach are the Vector Evaluated Genetic Algorithm (VEGA), Lexicographic ordering, Game Theory-based GAs. Again, References [3] and [18] analyze more deeply techniques based on this approach.

According to [18], until 1999 the number of published researches about MEAs was around 450 (based on [3]). Using the same source [3], this number is greater than 1,800 now (nov/2004), meaning that in the past five years the number of published researches about MEAs has quadruplicated. It also means a huge expansion in MEAs research field. Most of the new MEAs produced in this period are special versions of GAs (Genetic Algorithms), making the GAs the most used approach to such class of optimization problems. GAs are very popular optimization algorithms, with widespread usage as solvers for a great variety of problems. Almost all of them share as a characteristic the use of at least three algorithm parameters (e.g., population size, crossover rate, mutation rate) that must be fine tuned, in order to yield good performance. The multiobjective versions of GAs, here called M-GAs, usually have at least one more parameter (the niching or sharing parameter) [8], [18].

Like the GAs, GEO is a global search method [14], [16]. It is based on a simplified model of natural evolution, which was developed to show the emergence of Self-Organized Criticality (SOC) in ecosystems [1]. GAs and GEO are specially indicated to be used in complex optimization problems. They do not make use of derivatives and can be applied to constrained or unconstrained problems, non-convex or even disjoint design spaces, with any combination of continuous, discrete or integer variables.

Unlike the GAs, GEO has only one free parameter (τ) to adjust, making it easier to be fine tuned. The τ parameter allows the user to establish the determinism degree of the search, from a random walk, with $\tau=0$, where all moves have the same probability to happen, to a greedy search, with $\tau \rightarrow \infty$, where the best point found at each algorithm iteration is always used as a move by the algorithm. It has been observed that there exists an optimum τ value for each problem (sometimes a range), such that the global search efficiency is maximized. Most of the problems dealt with by GEO had their optimum τ values in the 1 ~ 5 interval [6], [14], [15], [16].

The multiobjective version of the Generalized Extremal Optimization (GEO), called M-GEO, keeps just the τ parameter to be adjusted.

The rest of the paper is organized as follows: Section 2 exposes with more details the M-GEO algorithm. Section 3 presents a description of the MAPSAR satellite, while Section 4 gives information about the kind of constellation we want to design. In Section 5, the two-objective problem is formulated, followed, in Section 6, by the results. In Section 7, the conclusions are presented.

2. THE MULTIOBJECTIVE GEO (M-GEO)

A flowchart of the M-GEO algorithm is presented in Figure 1. It does not make use of any kind of aggregation of the objective functions. It belongs to the third approach described in Section 1, the non-Pareto approach. In essence, the multi-objective strategy of M-GEO is the strategy of an n-to-one tournament, where, at each algorithm iteration, all the NFOBJ objective functions compete for the privilege of being used as the fitness assignment function and just one is chosen. As the choice is totally random, theoretically, any sequence of choices is possible, even those where only one objective function is used as the fitness assignment function during the entire search. This randomness allows M-GEO to access the entire Pareto frontier. The expected efficiency of the algorithm relies on the selection pressure imposed by the τ parameter over all objective functions, which "pushes" the algorithm movements in the objective space towards the Pareto frontier. In the following, the M-GEO steps presented in the flowchart of Figure 1 are described. Regarding the similarity of M-GEO and GEO, the second can be obtained from the first just imposing NOBJ=1 in flowchart of Figure 1. In that case, step 3 becomes redundant and can be omitted. Besides, allusions to "Pareto frontier" and "Pareto set" can be read as "best F(**X**)" and "**X** vector that leads to best F(**X**)", respectively.

1. Initialize randomly a population (string) of L species (bits) that encodes N design variables (**X** vector).

2. Flip all the L bits of the string, one at a time, generating L vectors X_b, $b \in \{1,2,...,L\}$ and calculates [$F_1(X_b)$, $F_2(X_b)$, ..., $F_{NFOBJ}(X_b)$] L times. Verify and save the Pareto frontier and the Pareto set

3. Choose randomly, among all NFOBJ objective functions, $F_I(\mathbf{X})$, $I \in \{1,2,..., NFOBJ\}$ one as I_c.

4. For each bit $b \in \{1,2,...,L\}$ attribute a fitness value proportional to the gain or loss that the I_c-th F(**X**),

5. Rank the bits, from 1 to L, according to their fitness values, generating a set of L couples (b,k), where b is the bit position on the string and k is its rank. The bit with the worst fitness has k=1.

6. Mutate one bit of the population with probability given by $P_k \propto k^{-\tau}$, $k \in \{1,2,...,L\}$.

7. Stopping criterion satisfied?

No

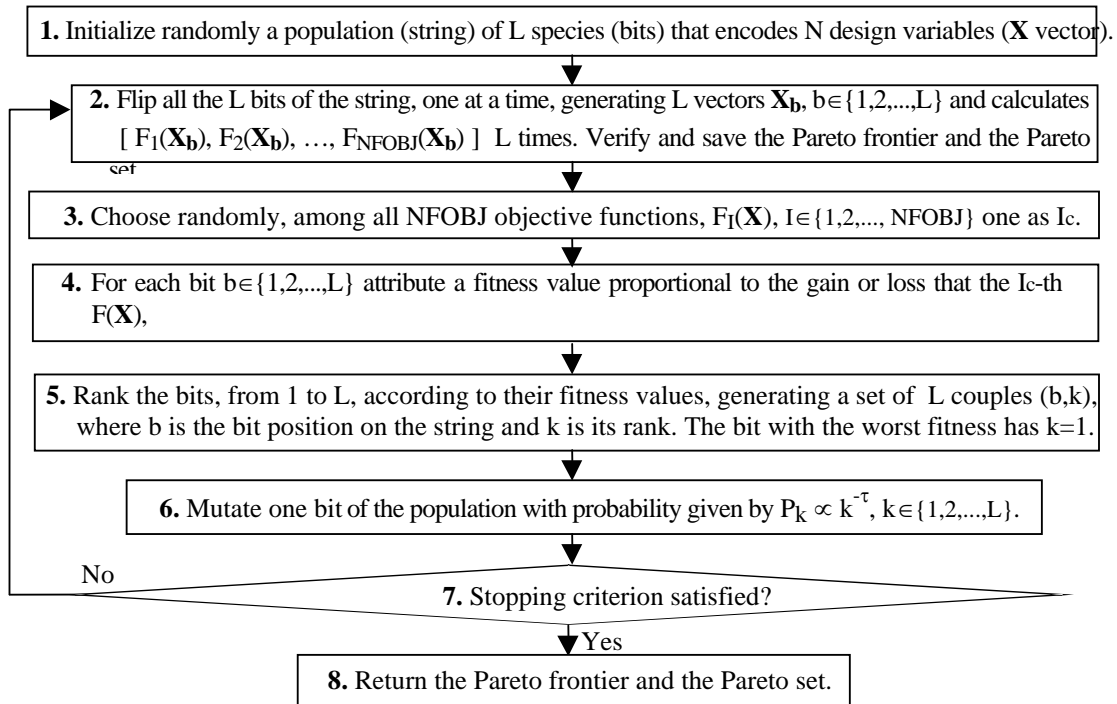**8.** Return the Pareto frontier and the Pareto set.

Yes

Figure 1. The M-GEO algorithm.

The first step of M-GEO is identical to the first step of GEO: a string of L bits is randomly filled with 0s and 1s. In the second step, all the L bits are flipped, one at a time, generating L different vectors in the search space, X_b, $b \in \{1,2,...,L\}$. "One at a time" means that before the next bit being flipped, the previous one is turned back to its original condition. All the NFOBJ objective functions are evaluated for all the X_b vectors, generating L objective function vectors of the form [$F_1(X_b)$, $F_2(X_b)$,..., $F_{NFOBJ}(X_b)$]. Still in the second step, the set containing the Pareto frontier approximation is created, verified, changed and saved, as necessary. In the third step, an objective function among all NFOBJ is randomly chosen. Once an objective function I_c is chosen, the search occurs (from the fourth to the seventh box in Figure 1) exactly as it happens in a GEO search, where the τ parameter imposes the selection pressure on the population individuals (the L bits and their L X_b associated vectors), based on their fitness regarding the objective function. One of the individuals is chosen (the associated bit is mutated), defining in this way, the movement of the algorithm in the search space. Posing it in a stepwise manner, in the fourth step, to each one of the L bits (and their associated X_b vectors) a fitness value is attributed, based on the gain or loss the I_c-th objective function has if the respective bit mutates, compared to the best value found so far for the I_c-th objective function. Mathematically, the fitness value is obtained by calculating the difference $\Delta F = F_{Ic}(X_b) - \text{best } F_{Ic}(\mathbf{X})$, $b \in \{1,2,...,L\}$, where "best $F_{Ic}(\mathbf{X})$" is the "best so far" value of $F_{Ic}(\mathbf{X})$ mentioned and it is the best value of $F_{Ic}(\mathbf{X})$ found during the search until the previous iteration of the algorithm

(steps **2.** through **7.**). For a minimization problem, negative values of ΔF mean poorly adapted species (bits), because flipping one of these bits leads to better designs. Then, in the fifth step, all the bits are ranked according to their fitness values, from 1 to L, generating a set of couples (b,k), where b is the bit linear position on the string and k is its respective rank. The bit with the worst fitness has k=1 and the bit with the best fitness has k=L. For minimization problems, the bit with the most negative or with the least positive ΔF has rank k=1, while for maximization problems the bit with the most positive or with the least negative ΔF has rank k=1. Next, in the sixth step, one bit, b_{chosen}, is chosen and mutated, according to a probability given by $P_k \propto k^{-\tau}$. In the present version of M-GEO, the task of the sixth step is accomplished by means of two drawings with uniform distribution. The first drawing chooses a value for k and $P_k = k^{-\tau}$ is calculated. Then, the second drawing returns a value within 0~1. If this value is equal or smaller than P_k, the k-th ranked bit is mutated. These two drawings are repeated as many times as needed until one bit is mutated. When a bit is mutated, it turns to be the b_{chosen} bit and the sixth step is done. In the seventh step, the stopping criterion is verified; if it holds the Pareto frontier found is retrieved and the algorithm terminates. If does not, the algorithm goes back to the second step and starts another iteration of the algorithm.

3. MAPSAR SATELLITE

The MAPSAR - *Multi-Application Purpose Synthetic Aperture Radar* satellite [12] has a Synthetic Aperture Radar (SAR) as its payload. The radar antenna has an elliptical parabolic main reflector with 7.5m length in azimuth and 5m width in elevation. The foreseen resolutions are 3m, 10m and 20m. It must be placed into a sun-synchronous orbit altitude between 600km and 650km. The most recent information indicates a 7-day cycle with 104 phased orbits (606km). After seven days, the cycle repeats itself, with the 105-th orbit being equal to the first one, regarding the resulting (ground) track on Earth's surface. The ground tracks are characterized by their fixed longitudes and constant inter-distances at the equator. The distance between adjacent ground tracks (the inter-track distance) is 385.3km for the 7-day cycle and two successive orbits produce ground tracks 2697.4km apart. The result is a "closed" (relatively to the Earth's surface) orbital grid of 104 orbits/ground tracks. Figure 2 presents a view of the MAPSAR satellite and Figure 3 shows the coverage geometry of its on-board SAR sensor. The image acquisition occurs in a plane, here called acquisition plane, which is perpendicular to the satellite Nadir ground track. The sensor is "blind" to a region defined by incidence angles (see Figure 3) between 0° and 20°, on both sides of the satellite Nadir track. This region, called the Nadir Zone, is indicated by a dotted line in Figure 3. The entire access region (thick green lines) is defined by incidence angles between 20° and 48.1^o, at both sides of the Nadir track. It should be noticed that the SAR antenna design allows the sensor to reach instantaneously (swath) only an extent up to 55 km approximately, inside the whole access regions of 395 km showed in Figure 3.
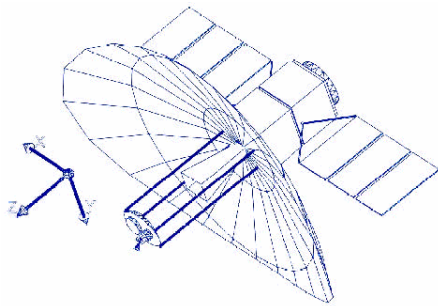

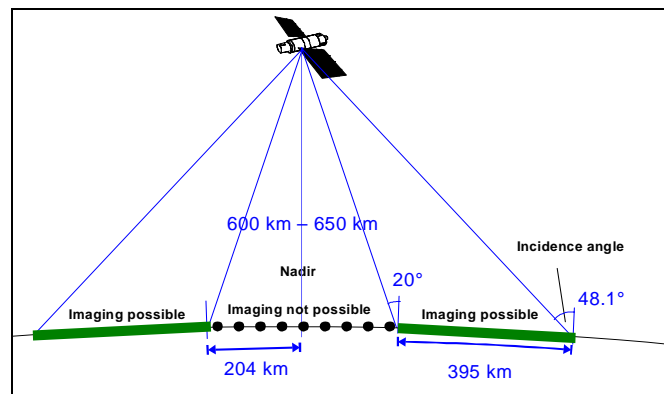Figure 2. Perspective view of MAPSAR
Source: [12].

Figure 3. Reach (20° a 48.1^o) of the SAR sensor
Source: adapted from [12].

4. MAPSAR CONSTELLATION

It is very common to choose sparse coverage constellation from the so-called Walker constellations. Unfortunately, this approach does not allow the establishment of compromise relations between both average and maximum revisit time, for constellation design purposes. Besides, Walker constellations impose that only symmetric constellations are considered in the search and it has been shown that this frequently prevent reaching the optimum constellation design [4], [7]. In the present study, Walker constellations were not used as a priori information (or imposition) to the design process.

Recapitulating and complementing the information given in Section 1, the constellation design study is carried out considering 2, 3 and 4 satellites. In all three cases, it is composed by the original MAPSAR satellite with its sun-synchronous orbit and 1, 2 or 3 more MAPSAR type satellites. The orbital parameters of the first satellite are fixed and serve as references to configure the rest of the constellation. The keplerian elements used

for the MAPSAR reference satellite are: semi-major axis (6,989.483km); eccentricity (0.0011); inclination (97.7722º); right ascension of the ascending node (230.962º); perigee argument (90º) and mean anomaly (90º).

The design variables for the remaining satellites are: inclination; ascending node right ascension and mean anomaly. The others orbital parameters are constant and equal to those of the reference satellite: semi-major axis (6,989.483km); eccentricity (0.0011) and perigee argument (90º).

The search for the constellation optimum design is done for the numbers of satellites previously mentioned. The satellites orbit simulation, with the state vector propagation, is carried out by a computer program developed specifically to the orbit propagation of multiple satellites. It is based on the orbital dynamics routines (in Fortran) developed at INPE by the orbital dynamics group for the propagation of just one satellite. Similarly to what was done in [17], the propagation is done considering only the effect of the Earth's gravitational field modeled by a central force field (mass point) plus the second zonal harmonic, J_2, which models the poles' flatness.

The region of interest is defined by the point coordinates: longitude (-62º) and latitude (-6º). It is located in the central portion of the Brazilian Amazon. Figure 4 shows it at the center of two concentric circles. The coordinates define a target point over which the maximum and the average revisit times are calculated and used as objective function values to the optimum constellation design with M-GEO. This calculus must take into account the image acquisition restrictions imposed by the SAR sensor limitations.
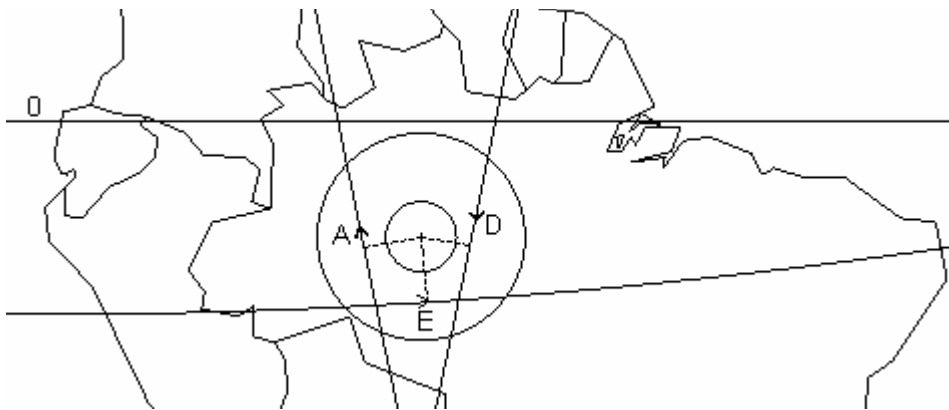

Figure 4. Visibility circles of the target point (Brazilian Amazon) and three ground tracks examples.

The visible passes of a satellite over a ground station are characterized by a set of azimuth and elevation angles, used to point the station antenna into the satellite direction, while the satellite moves on. The elevation angle is the one formed between the local horizontal plane and the line connecting the ground station and the satellite. A visible pass occurs whenever the elevation angle is greater than zero. As mentioned in Section 3, the whole access region of the MAPSAR sensor is defined by incidence angles between 20º and 48.1º. For a given point, the incidence angle and the elevation angle are quadrant complements, that is, the point with 20º incidence angle "sees" the satellite with an elevation angle of 90º-20º=70º, while the 48.1º point does the same with an elevation angle of 90º-48.1º=41.9º. Then, for a point on Earth's surface which is inside the acquisition plane of MAPSAR, if the elevation angle of the MAPSAR satellite at that point is greater than 41.9º and smaller than 70º, the point is inside the imaging access region of the MAPSAR sensor. In terms of ground tracks, this is equivalent to the two concentric visibility circles shown in Figure 4, one with radius of 204 km and other with 599 km. When the satellite ground track passes inside the outer circle and do not cross the inner circle, an image of the target point can be taken, meaning that a revisit has occurred. The image acquisition moment occurs when the acquisition plane of Figure 3 contains the target point (circles' center). At that moment, the situation is like the one shown in Figure 3. Therefore, if the ground distance between the satellite Nadir track (ground track) and the target point is lesser than 204 km, the target point is inside the Nadir Zone and the image can not be made. On the other hand, if the distance is greater than 204+395= 599 km, the target point is out of range and the image can not be made either. In Figure 4, the two concentric circles are representative of these restrictions, regarding any satellite (Nadir) ground track. Figure 4 illustrates also three satellite ground tracks that allow the radar imaging of the target point. It happens because at the image acquisition moment, indicated by the dotted lines, the satellite ground track is inside the outer circle and outside of the inner circle. The arrows indicate the satellite movement direction. The "A" labeled ground track is the ascendant part of one of the MAPSAR like reference orbits (sun-synchronous), while the "D" labeled is a descendant one. The "E" labeled ground track is the ascendant part of a near-equatorial orbit, with inclination around 10º and other parameters similar to the MAPSAR reference orbit.

During the orbit propagation, the following strategy is used to verify if a revisit has occurred. All passes whose elevation angles are greater than 41.9º are monitored and the corresponding elevation values are stored. Immediately after such passes, the maximum elevation value is verified. If it is smaller than 70º, a revisit is computed. The maximum elevation angle is used because it defines the instant in which the target point is inside the

the satellite acquisition plane. In a slightly more detailed manner, at each propagation step the elevation angle of the satellite regarding the target point is calculated. If it goes over 41.9^o, the elevation angles of the subsequent steps are stored until the end of the pass, that is, until the elevation goes under 41.9^o again. When that happens, the greatest value of the stored set is retrieved and if it is lesser than 70°, a revisit is computed with the update of the average and maximum revisit times.

5. MULTIOBJECTIVE OPTIMIZATION PROBLEM FORMULATION

Mathematically, the problem can be posed as:

Minimize $\mathbf{F}(\mathbf{X}) = [\ F_1(\mathbf{X})\quad F_2(\mathbf{X})\ ]$

Subject to: $\mathbf{X_{MIN}}\ \leq\ \mathbf{X}\ \leq\ \mathbf{X_{MAX}}$

(1)

where $F_1(\mathbf{X})$ is the average revisit time and $F_2(\mathbf{X})$ is the maximum revisit time over the target point. The objective is to minimize both $F_1(\mathbf{X})$ and $F_2(\mathbf{X})$, getting the Pareto frontier and the respective design solutions. The design variables are represented by the $\mathbf{X}$ vector in the optimization process. The vectors $\mathbf{X_{MIN}}$ and $\mathbf{X_{MAX}}$ contain the side constraints to each one of the variables, establishing their admissible ranges. The number of design variables is different for each one of the three constellation sizes (number of satellites on it) under investigation. These constellations, called constellations 1, 2 and 3 from now on, have the $\mathbf{X}$ vector as described on Table 1.

Table 1. Variables for optimization.

Constella-tion	X	Variable	Description	Satellite	Allowable Range $X_{MIN} \sim X_{MAX}$
1	1	I_2	Inclination	2	$0 \sim 20°$
	2	$\Omega_2\text{-}\Omega_1$	Right ascension phasing	2	$0 \sim 360°$
	3	$M_2\text{-}M_1$	Mean anomaly phasing	2	$0 \sim 360°$
2	1	I_2	Inclination	2	$0 \sim 20°$
	2	I_3	Inclination	3	$0 \sim 20°$
	3	$\Omega_2\text{-}\Omega_1$	Right ascension phasing	2	$0 \sim 360°$
	4	$\Omega_3\text{-}\Omega_1$	Right ascension phasing	3	$0 \sim 360°$
	5	$M_2\text{-}M_1$	Mean anomaly phasing	2	$0 \sim 360°$
	6	$M_3\text{-}M_1$	Mean anomaly phasing	3	$0 \sim 360°$
3	1	I_2	Inclination	2	$0 \sim 20°$
	2	I_3	Inclination	3	$0 \sim 20°$
	3	I_4	Inclination	4	$0 \sim 20°$
	4	$\Omega_2\text{-}\Omega_1$	Right ascension phasing	2	$0 \sim 360°$
	5	$\Omega_3\text{-}\Omega_1$	Right ascension phasing	3	$0 \sim 360°$
	6	$\Omega_4\text{-}\Omega_1$	Right ascension phasing	4	$0 \sim 360°$
	7	$M_2\text{-}M_1$	Mean anomaly phasing	2	$0 \sim 360°$
	8	$M_3\text{-}M_1$	Mean anomaly phasing	3	$0 \sim 360°$
	9	$M_4\text{-}M_1$	Mean anomaly phasing	4	$0 \sim 360°$

Note: Ω_1 and M_1 belong to the satellite 1 (reference satellite) and are constants.

Except for the inclination, all design variables are defined by the difference from the correspondent reference orbital parameter of satellite 1. It seems to be helpful to visualize the obtained constellations by directly comparing the angular displacements relatively to the reference satellite.

For a given $\mathbf{X}$, the respective keplerian elements of all satellites are calculated and also the corresponding state vectors. The satellite orbits are then propagated for a period of seven days with a step of 30 seconds. At the end, the final values for $F_1(\mathbf{X})$ and $F_2(\mathbf{X})$ are returned (the forward model of the problem). The $\mathbf{X}$ values are generated by M-GEO, during its search, and then passed to the orbit propagation program, which is coupled to M-GEO. All design variables were encoded using 8 bits, which means a resolution of $0.078°$ for the inclination and $1.406°$ for the other design variables. The allowable range for the inclination was shortened from $0\sim180°$ to $0\sim20°$ because, as the target point is near equatorial ($-6°$ in Latitude), it was clear that the near equatorial inclination would have better performance, in terms of revisit time.

6. RESULTS

The M-GEO algorithm was run for each Constellation described in the previous Section. For each run, 25 different seeds (random **X** vectors) were used to restart the search. For each seed, 10,000 evaluations of $F(X) = [F_1(X) \ F_2(X)]$ were allowed and this was used as stopping criterion. During all the time, the Pareto frontier was stored and updated. This way, the search for the Pareto frontier of each constellation used 250,000 evaluations of $F(X)$. Different seeds were used in order to generate results that are robust from a statistical viewpoint. For all three runs $\tau=2$ was used. For the "heaviest" problem of Constellation 3, the computation time was around 3 days in a Intel Pentium 4 2.6GHz PC with 512MB RAM.

Figures 5 through 7 give the Pareto frontiers for the Constellations 1 to 3, respectively. The points of the approximate Pareto frontier obtained with M-GEO are line connected for visualization purposes. For the first Constellation, only five different design solutions were found for the Pareto set, leading to a Pareto frontier of four points. For the second Constellation, 26 different design solutions were found for the Pareto set, leading to a Pareto frontier with 20 points. For the third Constellation, 10 different design solutions and Pareto frontier points were found.

What is readily seen in these figures is that an optimization only of the average revisit time $F_1(X)$ leads to a huge deteriorating of the maximum revisit time $F_2(X)$. On the other hand, optimization only of the maximum revisit time $F_2(X)$ leads to a slight worsening of the average revisit time $F_1(X)$. A similar behavior was observed in [17], where constellations for sparse global coverage were studied. This is an important result, because it suggests that when dealing with single-objective optimization of these constellation types, to use the maximum revisit time as criterion is preferable.
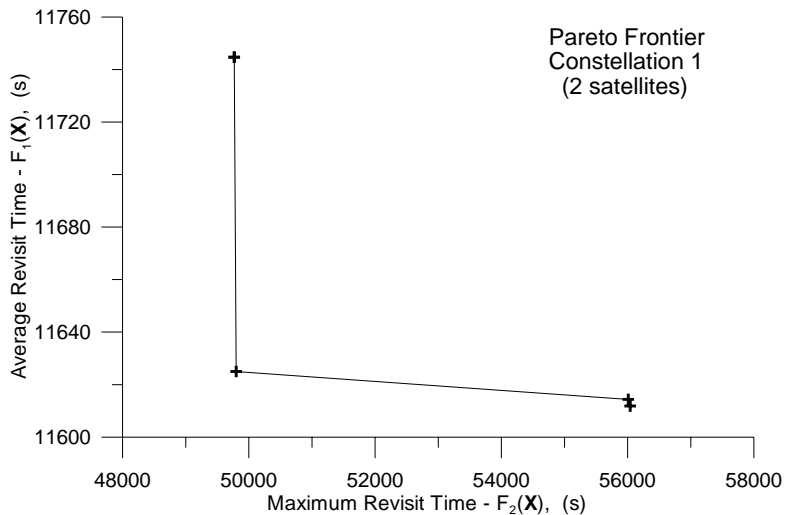

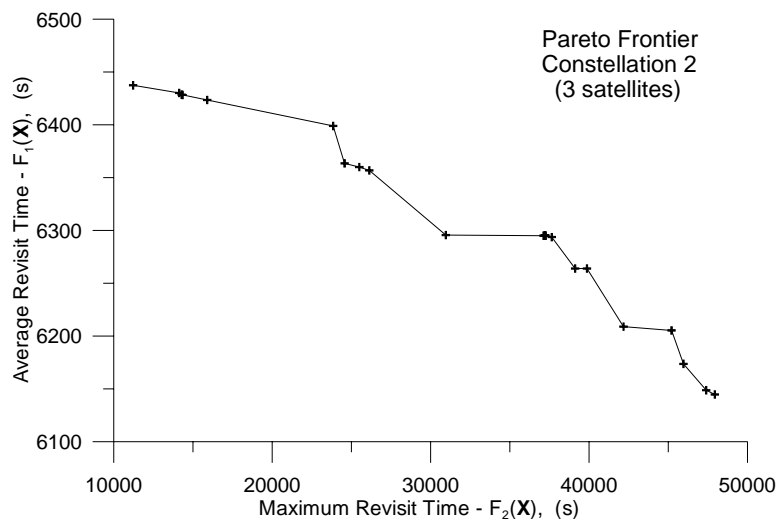
Figure 5. Pareto frontier of Constellation 1.

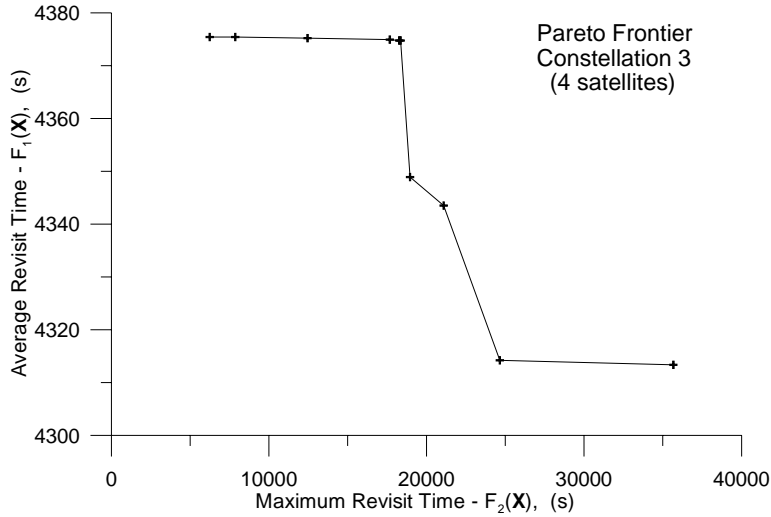Figure 6. Pareto frontier of Constellation 2.

Figure 7. Pareto frontier of Constellation 3.

In Table 2, the set of solutions (**X** vectors) found for all points (values in bold) of the Pareto frontier of Constellation 1 are presented, while Tables 3 and 4 do the same for Constellations 2 and 3, respectively, but for selected points.

Table 2. Constellation 1 solutions for all points of the Pareto frontier.

I_2	$\Omega_2-\Omega_1$	M_2-M_1	F_1	F_2
3.76	272.5	63.5	**11744.7**	**49770.0**
3.84	272.5	63.5		
4.16	272.5	77.6	**11625.0**	**49800.0**
4.24	285.2	94.6	**11614.4**	**56010.0**
4.24	285.2	101.6	**11611.9**	**56040.0**

Table 3. Constellation 2 solutions for three points of the Pareto frontier.

I_2	I_3	$\Omega_2-\Omega_1$	$\Omega_3-\Omega_1$	M_2-M_1	M_3-M_1	F_1	F_2
4.16	4.16	187.8	360.0	328.9	86.1	**6437.4**	**11220.0**
3.92	4.16	211.8	114.4	334.6	83.3	**6295.6**	**30960.0**
4.16	4.16	266.8	276.7	117.2	360.0	**6144.7**	**47940.0**

Table 4. Constellation 3 solutions for four points of the Pareto frontier.

I_2	I_3	I_4	$\Omega_2-\Omega_1$	$\Omega_3-\Omega_1$	$\Omega_4-\Omega_1$	M_2-M_1	M_3-M_1	M_4-M_1	F_1	F_2
4.00	4.08	3.84	355.8	240.0	121.4	168.0	343.1	98.8	**4375.4**	**6240.0**
4.00	4.00	3.69	148.2	64.9	218.8	76.2	88.9	276.7	**4374.8**	**18360.0**
4.00	4.08	3.84	176.5	240.0	111.5	32.5	338.8	121.4	**4314.2**	**24660.0**
4.00	4.00	3.69	148.2	132.7	207.5	76.2	83.3	271.1	**4313.4**	**35670.0**

From Tables 3 and 4 is possible to observe a common pattern, where the satellites are almost uniformly distributed in $\Omega_j-\Omega_1$, $j \in \{2,3,4\}$, in respect to the best value of F_2 of the Pareto frontier, while they are much closer to each other in respect to the best value of F_1. For instance, taking the best in F_2 solutions as reference and explicating a bit more what was just said, for Constellation 2, with best $F_2=11220$, it means $(\Omega_3-\Omega_1)-(\Omega_2-\Omega_1)$ $= 360.0°-187.8°= 172.2°$, which is close to the uniform distribution of $360°/2=180°$ for two satellites. For Constellation 3, with best $F_2=6240$, it means $(\Omega_2-\Omega_1)-(\Omega_3-\Omega_1) = 355.8°-240.0°= 115.8° \cong (\Omega_3-\Omega_1)-(\Omega_4-\Omega_1) = 240.0°-121.4°= 118.6° \cong (\Omega_4-\Omega_1)-(\Omega_2-\Omega_1) = 121.4°-355.8° = -234.4° = 125.6°$, that is close to the uniform distribution of $360°/3=120°$ for three satellites. In contrast, now taking the best in F_1 solutions, the maximum difference $(\Omega_j-\Omega_1)- (\Omega_k-\Omega_1)$, $\forall j\neq k$, j and k $\in \{2,3,4\}$ was 9.9° for Constellation 2 and 74.8° for Constellation 3.

In Figures 8 to 10, curves showing the average behavior (over the 25 seeds) for Best $F_1(\mathbf{X})$ and for Best $F_2(\mathbf{X})$ are plotted for the Constellations 1, 2 and 3. Additionally, the best and the worst seed curves within the 25 are also plotted. Looking at Figures 8a and 8b, it is possible to consider that for Constellation 1, the average evolu-

tion of $F_1(\mathbf{X})$ and $F_2(\mathbf{X})$ practically stabilizes after 6,000 evaluations. The same seems to happen after 7,000 evaluations for Constellation 2 and after 4,000 for Constellation 3.
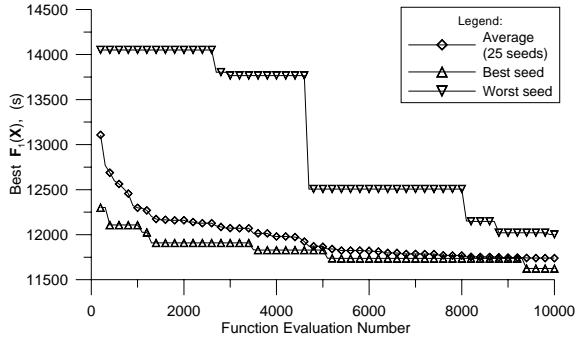

Figure 8a. $F_1(X)$ evolution (Constellation 1).

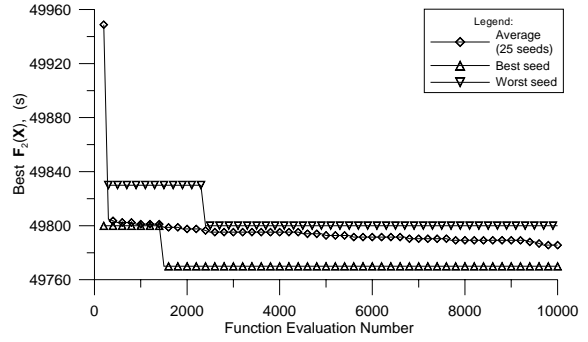Figure 8b. $F_2(X)$ evolution (Constellation 1).

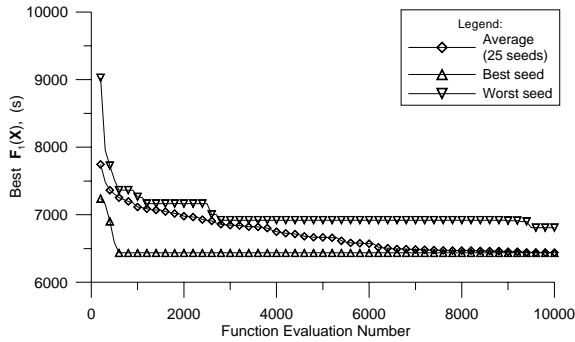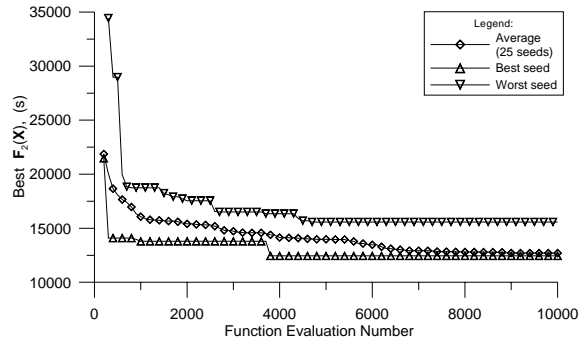Figure 9a. $F_1(X)$ evolution (Constellation 2).
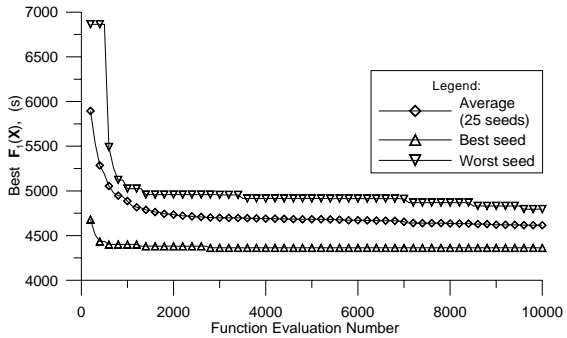

Figure 9b. $F_2(X)$ evolution (Constellation 2).

Figure 10a. $F_1(X)$ evolution (Constellation 3).
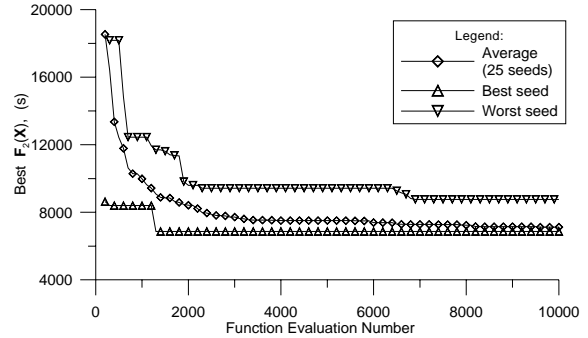

Figure 10b. $F_2(X)$ evolution (Constellation 3).

7. CONCLUSIONS

This paper has described an application of a multiobjective version of the GEO algorithm (M-GEO) to the inverse design of a remote sensing constellation based on the MAPSAR satellite. The most important conclusion is that the objectives were successfully achieved, with the M-GEO algorithm being able to generate the approximate Pareto frontier for the problem, obtaining the associated design solutions. The results indicate that with just two satellites it is possible to have both global coverage and a maximum revisit time over the target point of 49770 s, that is, 13.825 hours, less than one day, as aimed for disaster monitoring. Such a good performance result was achieved partly due the fact that the target point is near equatorial. Revisit studies over points in higher latitudes and for the same number of satellites would certainly yield worst performance results. Additional studies for target points on higher latitudes and also for regions defined by a grid of points are being considered, thus extending the method described herein.

REFERENCES

1. P. Bak and K. Sneppen, Punctuated equilibrium and criticality in a simple model of evolution. *Physical Rev. Lett.* (1993) **71**(24), 4083-4086.

2. C.A.C. Coello, *Evolutionary Multiobjective Optimization (EMOO)*, Web page. www.lania.mx/~ccoello/EMOO/, 2004.

3. C.A.C. Coello, A comprehensive survey of evolutionary-based multiobjective optimization techniques, *Knowledge and Information Systems. An International Journal* (1999) **1**(3), 269-308.

4. W.A. Crossley and E.A.Williams, Simulated annealing and genetic algorithms approaches for discontinuous coverage satellite constellation design. *Engineering Optimization* (2000) **32**, 353-371.

5. C.M. Fonseca and P.J. Fleming, An overview of evolutionary algorithms in multiobjective optimization. *Evolutionary Computation* (1995) **3**(1), 1-16.

6. R.L. Galski, F.L. Sousa, F.M.Ramos and I. Muraoka, Spacecraft thermal design with the generalized extremal optimization algorithm. *Proceedings of the Inverse Problems, Design and Optimization Symposium*, Rio de Janeiro, 2004, cd-rom.

7. E. George, Optimization of satellite constellations for discontinuous global coverage via genetic algorithms. *Proceedings of AAS/AIAA Astrodynamics Specialist Conference*, Sun Valley, ID, USA, 1997. (AAS 97-621).

8. A. Goicoechea, D.R. Hansen and L. Duckstein, *Multiobjective Decision Analysis with Engineering and Business Applications*, John Wiley and Sons, New York, 1982.

9. D.E. Goldberg, *Genetic Algorithms in Search, Optimization and Machine Learning*. Addison-Wesley, Massachusetts, 1989.

10. A. Messac, G.J. Sundararaj, R.V. Tappeta and J.E. Renaud, Ability of objective functions to generate points on nonconvex Pareto frontiers. *AIAA J.* (2000) **38**(6), 1084-1091.

11. K. Miettinen, Some Methods for Non-linear Multi-objective Optimization*, Lecture Notes in Computer Science: Evolutionary Multi-Criterion Optimization*, v1993, 2001, pp. 1-20.

12. R. Schröder, J. Puls, I. Hajnsek, F. Jochim, T. Neff, J. Kono, W.R. Paradella, M.M.Q. Silva, D.M. Valeriano and M.P.F. Costa, MAPSAR: A small L-band SAR mission for land observation. *Acta Astronautica J.* (2005) .**56**(1-2), 35-43.

13. Shapour, A. *Multiobjective Optimal Design*, University of Maryland at College Park, http://www.glue.umd.edu/~azarm/optimum_notes/multi/multi.html. 1996.

14. F.L. Sousa and F.M. Ramos, Function optimization using extremal dynamics*, Proceedings of the 4th International Conference on Inverse Problems in Engineering*, Rio de Janeiro, Brazil, 2002, cd-rom.

15. F.L. Sousa, F.M. Ramos, R.L. Galski and I. Muraoka, Generalized Extremal Optimization: A New Meta-heuristic Inspired by a Model of Natural Evolution. In*: Recent Developments in Biologically Inspired Computing*, De Castro, L. N. & Von Zuben, F. J. (editors), Idea Group Inc., 2004, pp. 41-60.

16. F.L. Sousa, F.M. Ramos, P. Paglione and R.M. Girardi, A new stochastic algorithm for design optimization. *AIAA J.* (2003) **41**(9), 1808-1818.

17. E.A. Williams, W.A. Crossley and T.J. Lang, Average and maximum revisit time trade studies for satellite constellations using a multiobjective genetic algorithm. *J. Astronautical Sci.* (2001) **49**(3), 385-400.

18. A. Van Veldhuizen and G.B. Lamont, Multiobjective evolutionary algorithms: Analyzing the state-of-the-art, *Evolutionary Computation* (2000) **8**(2), 125-147.